14

INJURY BIOMECHANICS RESEARCH
Proceedings of the Thirty-First International Workshop

Effect of Loading Rate on Compressive Failure Mechanics of the Pediatric Cervical Spine

P. Z. Elias, D. J. Nuckley, and R. P. Ching

ABSTRACT

This study investigated the effect of loading rate on the compressive failure mechanics of the pediatric cervical spine, using baboons of a controlled age group as a human surrogate. Cervical spines were obtained from 12 male baboons (9 ± 1 human equivalent years) and dissected into 35 2-FSU segments. All specimens underwent cyclic preconditioning to 100 N for 50 cycles at 1 Hz prior to failure testing at displacement rates of 5, 50, 500, or 5,000 mm/sec. Load-displacement curves were plotted and analyzed to determine stiffness, failure load, and displacement at failure for the various loading rates. Stiffness showed a significant increase as loading rate was increased, with mean stiffness increasing 30 % between rates of 5 and 5,000 mm/sec. Failure load showed an increasing, though not statistically significant, trend with increasing loading rate, while displacement at failure showed no rate dependence. The results of this research may be useful for developing better pediatric automotive safety standards, improved biofidelic test dummies, and more accurate computational models.

INTRODUCTION

To date, the effort towards prevention of pediatric cervical spine injuries has been hindered by a lack of data on pediatric spine mechanics. Although pediatric injuries to the cervical spine are not particularly common, they may be associated with significant rates of mortality and disability (Brown et al., 2001). To reduce such injuries, various crash-test dummies, computational models, and safety standards have been developed by scaling adult injury tolerance data to children. While animal models have been used to establish pediatric tensile (Ching et al., 2001, Pintar et al., 2000) and compressive (Nuckley et al, 2002a) scaling factors, the viscoelastic behavior of biologic tissues requires that loading rate be taken into account for a thorough understanding of cervical spine

mechanical properties. As such, this study aims to contribute data on the compressive failure mechanics of the cervical spine with an emphasis on the effect of loading rate.

The adult human cervical spine has been widely studied. Several groups have used full cervical spine preparations to investigate mechanical properties in compression (Panjabi et al., 1998, Pintar et al., 1998, Nightingale et al., 1996, Pintar et al., 1995a). Compressive tolerances and functional properties have been established, and the effect of loading rate has been documented. Pintar et al. (1995) reported a force at failure of 3.8 kN for adult males, and later showed significantly increasing mechanical properties with loading rate (1998). Full cervical spine preparations, however, make it difficult to apply a purely compressive load and to measure properties for different segments of the cervical spine.

Individual motion segments have also been used to study the adult cervical spine. Several studies have tested segments consisting of 2 function spinal units because they allow failure in the hard or soft tissues without buckling (Nuckley et al., 2002a, Carter et al., 2000, Zhu et al., 1999, Yingling et al., 1997, Pintar et al., 1995b). Of these studies, only Yingling et al. attempted to determine the effect of loading rate over a wide range of rates. Using a porcine model, Yingling et al. tested cervical spine segments at rates ranging from 100 to 16,000 N/s. However, the highest rate tested corresponded to a displacement rate of not more than 50 mm/sec, which is likely lower than the rates experienced in severe car crashes. Additionally, their data sampling rate of 50 Hz may have been inadequate for the higher rates.

A baboon model has been chosen because of both the demonstrated similarities between the baboon and human cervical spine (Tominaga et al., 1995, Swindler and Wood, 1973), and the scarcity of available healthy human pediatric tissues. Although baboons exhibit smaller size, thinner pedicles, and non-bifid spinous processes relative to humans, the geometry, anatomy, and mechanical properties compare very well overall. These characteristics, along with its phylogenetic proximity to humans, have made the baboon model an excellent human surrogate.

This study aims to test pediatric baboon cervical spine segments over a range of loading rates up to 5,000 mm/sec. With loading rates and sampling rates more than two orders of magnitude greater than Yingling et al, these tests will allow measurements in a scenario more similar to an actual car crash. This data on the compressive failure mechanics of the pediatric cervical spine may be useful in the development of better pediatric safety standards, computational models, and crash-test dummies.

METHODS

Specimen Preparation

Twelve fresh-frozen baboon cadavers were obtained through the University of Washington Regional Primate Research Center. All baboons were males of age 9 ± 1 human equivalent years, previously used and euthanized in unrelated studies not involving the musculoskeletal system. Human equivalent years were determined by using a CT scan in conjunction with a cervical spine maturation index that evaluates the 1st, 2nd, and 3rd cervical vertebrae for specific radiographic characteristics (Kuhns, 1998, Hassel and Farman, 1995).

Each specimen was inspected for spinal injury and pathology before gross dissection to remove musculature and other soft tissues. The remaining full and intact cervical spine was then dissected into 3 segments, each comprised of 2 functional spinal units (Occiput - C2, C3 - C5, or C6 - T1). A functional spinal unit (FSU) consists of 2 vertebrae and the disc, ligaments, and capsules between them. A total of 35 2-FSU segments were obtained for testing, with 1 segment lost due to dissection error.

Prior to testing, wires were passed through the vertebral body and lateral masses (Figure 1a) on both the superior and inferior sides of each spine segment for a total of 6 wires per specimen. Following wiring, each segment was embedded in polymethylmethacrylate (PMMA) to maintain proper orientation and position during load application (Figures 1b and 1c). Wiring provided more purchase for the test segment within the PMMA to ensure rigid fixation.

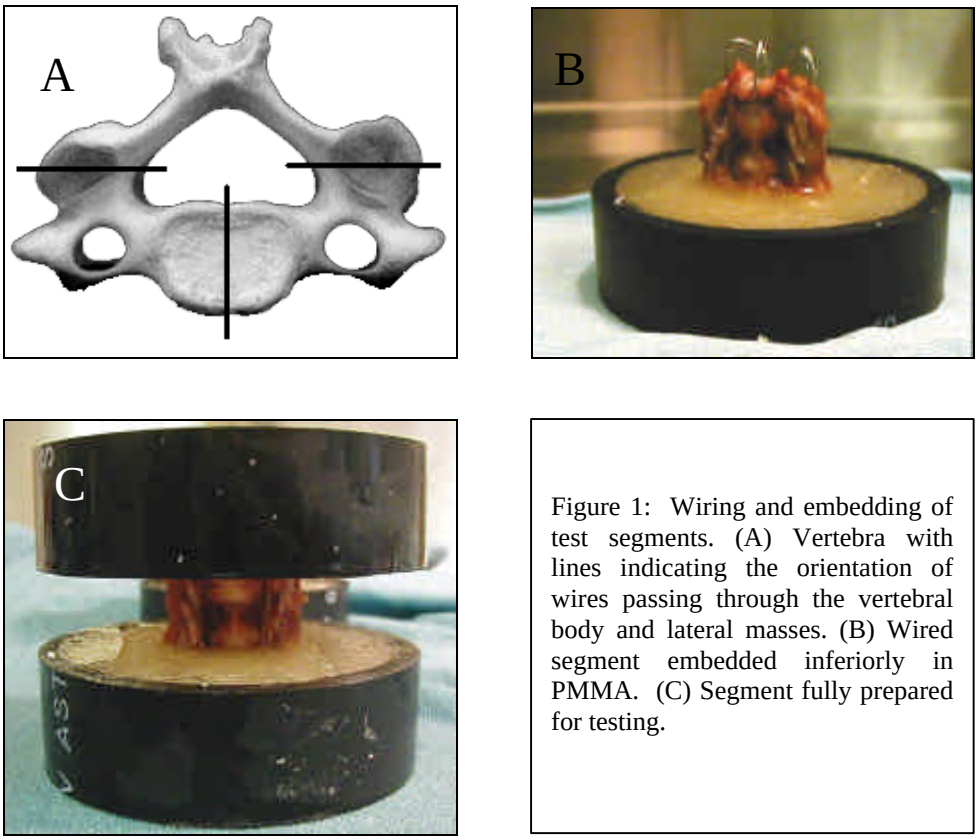

Figure 1: Wiring and embedding of test segments. (A) Vertebra with lines indicating the orientation of wires passing through the vertebral body and lateral masses. (B) Wired segment embedded inferiorly in PMMA. (C) Segment fully prepared for testing.

Testing Apparatus

Testing was conducted with a custom MTS (Model 858 Bionix, Material Tests System Corp., Minnesota) servohydraulic testing system (Figure 2a). Stiffness of the MTS frame and experimental testing apparatus was found to be more than 10 times greater than that of the stiffest specimen. Figure 2b shows a prepared segment within the MTS just prior to failure testing.

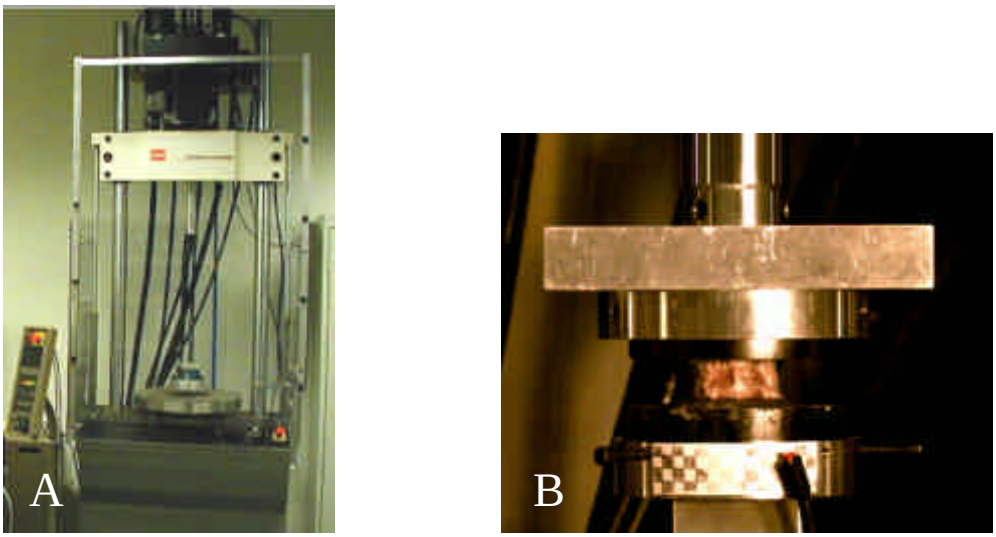

Figure 2: Experimental test apparatus. (A) Servohydraulic MTS capable of dynamic displacement inputs up to 10 m/s. (B) A C3-C5 segment attached to the MTS ram superiorly and to the six-axis load cell inferiorly.

Prepared test segments were secured to a 6-axis load cell inferiorly and superiorly to the MTS ram. Displacements were measured with a Linear Variable Differential Transformer (LVDT), and also via high-speed video camera. Load data was collected from the 6-axis load cell. Sampling rates for the LVDT and load cell ranged from 200 to 20,000 Hz, while the camera recorded at rates from 60 frames/sec to 4,000 frames/sec. Sampling rates and camera frame rates for each loading rate group are summarized in Table 1. LabVIEW data acquisition software (version 6.0, National Instruments, Texas) was used to record loads and LVDT displacements, while WINanalyze software (version 1.4, Mikromak, Germany) was used to obtain displacements from the high-speed video.

Table 1. Sampling Rates And Camera Frame Rates For Each Loading Rat E Group

Loading Rate (mm/s)	Sampling Rate (Hz)	Camera Frame Rate (F/s)
5	1,000	60
50	4,000	60
500	8,000	500
5,000	20,000	4,000

Testing Protocol

Each segment was randomly assigned to one of four loading rate groups (5, 50, 500, or 5,000 mm/sec), ensuring that each group contained three Oc-C2, three C3-C5, and three C6-T1 segments. The 5 mm/sec group, however, contained only two C6-T1 segments due to a dissection error. Segments were preconditioned 50 cycles at 1 Hz to a load of 100 N. Following preconditioning, each segment was failed in axial compression via a haversine displacement-controlled input at a rate of 5, 50, 500, or 5,000 mm/sec.

Data Analysis

The last load-displacement curve from each preconditioning cycle was plotted and stiffness was calculated as the slope of the linear region of the curve. For the failure testing, it was not possible to identify a single linear region in many of the load-displacement profiles. An average linear stiffness was therefore calculated by dividing the failure load by the displacement at failure, with displacement measured from the point where the specimen first began taking load. The circles shown in Figure 3 illustrate the failure load and the point of initial displacement. The slope of the line drawn to connect the two points represents the average linear stiffness.

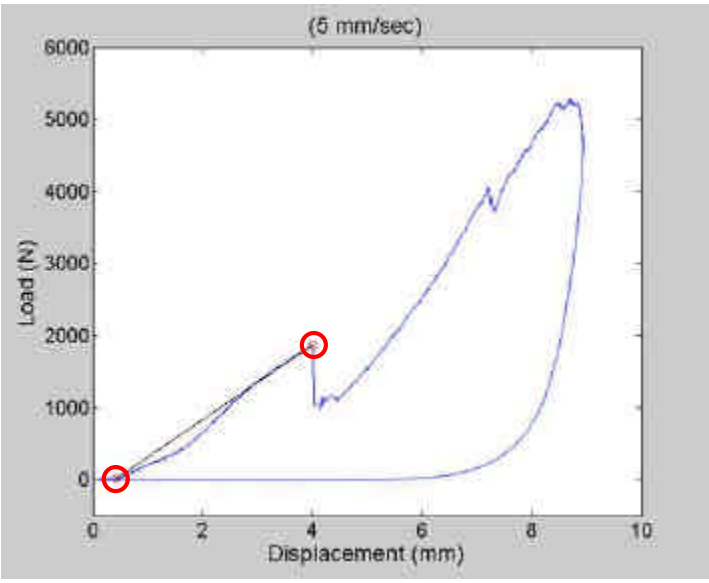

Figure 3: Representative load-displacement curve (Oc-C2).

Failure loads were determined by identifying the first sharp drop in load, accompanied by increasing displacement. This method aimed to consider only catastrophic damage as being indicative of failure, rather than sub-catastrophic injuries often apparent as small, sharp reversals in load, followed by very rapid re-establishment of stiffness.

Data filtering (Butterworth filter applied only to the preconditioning load-displacement curves), plotting, and analysis were performed with MATLAB software (version 5.3, MathWorks, Massachusetts), while statistics were calculated using SAS/STAT software (version 6.12, SAS, North Carolina).

RESULTS

Preconditioning

Mean stiffness, calculated as described from the preconditioning load-displacement profiles was 369 ± 72 N/mm for all specimens. ANOVA revealed no statistically significant difference in stiffness between the various loading rate groups ($p = 0.1709$).

Failure Tests

Stiffness was found to increase significantly with loading rate, as shown in Figure 4 ($p = 0.0379$). Mean stiffness increased by 30 % between the slowest and fastest loading rates. Individual contrasts between the 5 and 5,000, and 50 and 5,000 mm/sec groups were significant with $p < 0.0165$. Significant differences between loading rate groups are visualized by lack of overlap between the shaded areas of two boxes. The shaded areas represent two standards deviations (95% of the data) above and below the mean, which is indicated by the horizontal line within each box. Whiskers on each box reach to the farthest outliers, indicating the full range of the data.

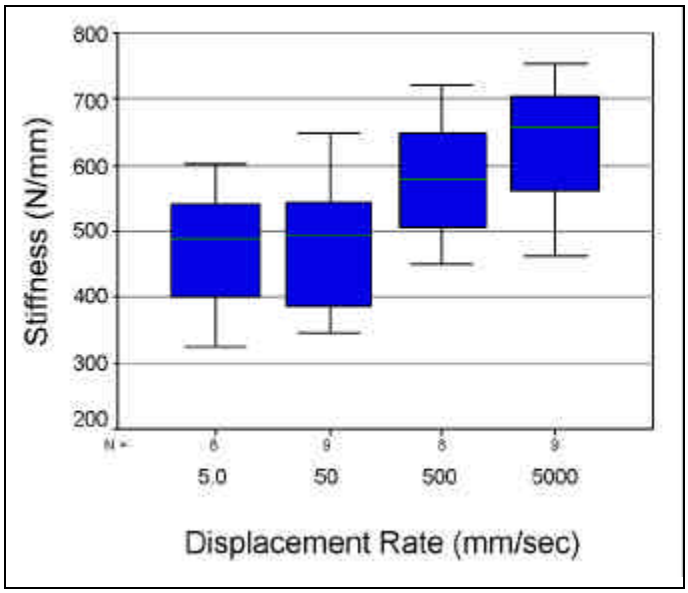

Figure 4: Stiffness vs. Displacement Rate ($p = 0.0379$).

A trend towards increasing failure load with increasing loading rate was observed as shown in Figure 5, but no statistical difference existed between the different loading rate groups. A power analysis suggested that with the given specimen variability, 9 additional specimens (27 FSUs) would make the observed trend statistically significant.

Displacement at failure was independent of loading rate, as shown in Figure 6 ($p = 0.8472$).

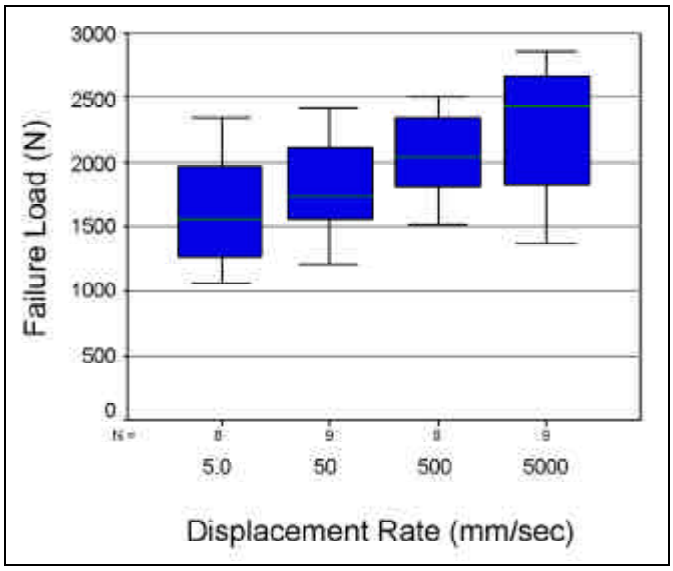

Figure 5: Failure Load vs Displacement Rate (p = 0.5575).

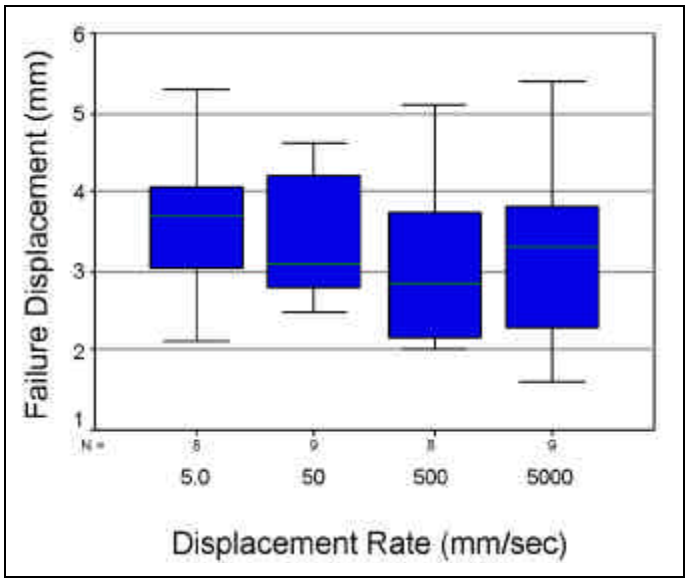

Figure 6: Failure Displacement vs. Displacement Rate (p = 0.8472).

Post-failure radiographs showed mostly general compression fractures for the 5 mm/sec tests, while the higher rates produced mostly burst fractures (Figure 7).

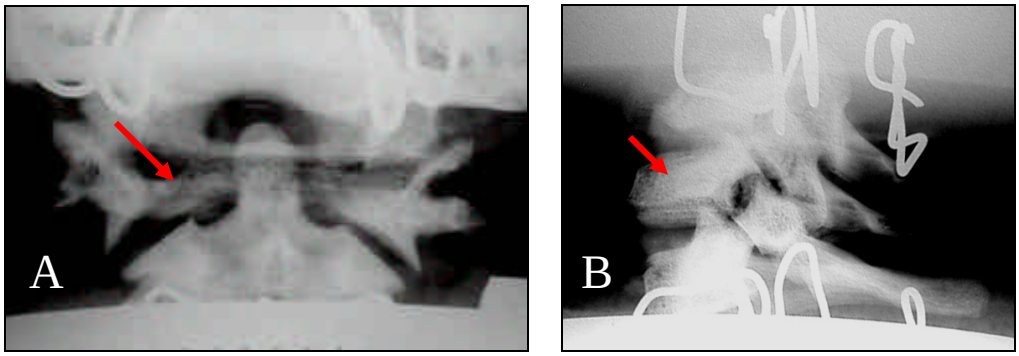

Figure 7: Post-injury radiographs. (A) Oc-C2 segment showing C1 burst fracture and separation of the C1-C2 facet. (B) C6-T1 segment exhibiting a C7 burst fracture with associated lateral mass fracture.

DISCUSSION

The preconditioning stiffness calculations showed that the specimens in the various loading rate groups exhibited similar stiffness at 1 Hz. It can therefore be concluded that there was no inherent bias in the loading rate groupings for the failure testing.

The increasing stiffness found with loading rate for the failure tests is consistent with the general viscoelastic behavior of biologic tissues (Danto & Woo, 1993, Neumann et al., 1994), and with previous literature on cervical spine motion segments (Yingling et al., 1997). These results are also consistent with tests conducted on thoracic (Kazarian and Graves, 1977) and lumbar (Hutton and Adams, 1982) spine motion segments, in which strain rate was varied.

The trend of increasing failure load with loading rate, without statistical significance, suggests that rate dependence may be strongest between quasi-static and dynamic rates, rather than between different dynamic rates (Yingling et al., 1997, Pintar et al., 1998). Yingling found that at loading rates from 1000 – 16,000 N/s, there was no statistically significant increase in failure load. While the failure load trend in this study appears stronger towards rate dependence, the effect of loading rate is clearly not extreme over the rates tested.

The rate independence shown for displacement at failure is consistent with tensile tests conducted by Nuckley et al. (2002b) at similar loading rates for the same age group. It appears that the failure mechanism in cervical spine segments is based on strain rather than stress.

The results of this research provide a set of cervical spine compressive injury tolerance data for a pediatric baboon population that can be scaled to the pediatric human population. The dynamic loading rates conducted for the failure testing simulate the range of rates seen in car crashes and illustrate the potential importance of loading rate in cervical spine injury.

CONCLUSIONS

This study aimed to determine the effect of loading rate on compressive failure mechanics of the pediatric cervical spine. It was found that stiffness increased significantly with loading rate, while displacement at failure was independent of rate. Failure load showed an increasing, but not statistically significant, trend with increasing loading rate. The results of this research may be useful for development of better pediatric automotive safety standards, improved biofidelic crash-test dummies, and more accurate computational models.

ACKNOWLEDGEMENTS

This research was funded by The National Center for Injury Prevention and Control, Centers for Disease Control. The National Highway Traffic Safety Administration also contributed to the success of this study. Special thanks to lab members Craig Chartier, Michael Dahl, Michael Eck, Allison Hoppe, Grace Ku, and Eno Yliniemi for their assistance throughout the project.

REFERENCES

BROWN, R. L., BRUNN, M. A., and GARCIA, V. F. (2001). Cervical spine injuries in children: A review of 103 patients treated consecutively at a level 1 pediatric trauma center. J Pediatric Surg, 36(8): 1107-1114.

CARTER, J. W., MIRZA, S. K., TENCER, A. F., and CHING, R. P. (2000). Canal geometry changes associated with axial compressive cervical spine fracture. Spine, 25(1): 46-54.

CHING, R. P., NUCKLEY, D. J., HERTSTED, S. M., ECK, M. P., MANN, F. A., and SUN, E. A. (2001). Tensile mechanics of the developing cervical spine. Stapp Car Crash J, 45: 329-336.

DANTO, M. I. and WOO, S. L. (1993). The mechanical properties of skeletally mature rabbit anterior cruciate ligament and patellar tendon over a range of strain rates. J Orthop Res, 11(1): 58-67.

HASSEL, B. and FARMAN, A. G. (1995). Skeletal maturation evaluation using cervical vertebrae. Am J Orthodontics and Dentofacial Orthopedics, 107(6): 19A.

HUTTON, W. C. and ADAMS, M. A. (1982). Can the lumbar spine be crushed in heavy lifting? Spine, 7: 586-590.

KAZARIAN, L. and GRAVES, G. A. (1977). Compressive strength characteristics of the human vertebral centrum. Spine, 2(1): 1-14.

KUHNS, L. R. (1998). Imaging of spinal trauma in children. An atlas and index. B.C. Decker, Inc., Hamilton, Ontario.

NEUMANN, P., KELLER, T. S., EKSTROM, L., and HANSSON, T. (1994). Effect of strain rate and bone mineral on the structural properties of the human anterior longitudinal ligament. Spine, 19(2): 205-211.

NIGHTINGALE, R. W., MCELHANEY, J. N., RICHARDSON, W. J., and MYERS, B. (1996). Dynamic responses of the head and cervical spine to axial impact loading. J Biomech, 29: 307-318.

NUCKLEY, D. J., HERTSTED, S. M., KU, G. S., ECK, M. P., and CHING, R. P. (2002a). Compressive tolerance of the maturing cervical spine. Stapp Car Crash J., 46: 431-440.

NUCKLEY, D. J. HERTSTED, S. M., and CHING, R. P. (2002b) Effect of strain rate on cervical spine tensile mechanics. World Congress of Biomechanics IV, Calgary, Alberta.

PANJABI, M. M., CHOLWICKI, J., NIBU, K., GRAUER, J., BABAT, L. B., and DVORAK, J. (1998). Critical Load of the human cervical spine. Clin Biomech, 13(1): 11-17.

PINTAR, F. A., MAYER, R. G., YOGANANDAN, N., and SUN, E. A. (2000). Child neck strength characteristics using an animal model. Stapp Car Crash J., 44: 77-83.

PINTAR, F.A., YOGANANDAN, N., and VOO, L. (1998). Effect of age and loading rate on human cervical spine injury threshold. Spine, 23(18): 1957-1962.

PINTAR, F. A., YOGANANDAN, N., VOO, L., CUSICK, J. F., MAIMAN, D. J., and SANCES, A. (1995a). Dynamic characteristics of the human cervical spine. Soc Auto Eng Trans, 104: 3087-3094.

PINTAR, F. A., YOGANANDAN, N., PESIGAN, M., REINARTZ, J., SANCES, A., JR., and CUSICK, J. F. (1995b). Cervical vertebral strain measurements under axial and eccentric loading. J Biomech Eng, 117(4): 474-478.

SWINDLER, D. R. and WOOD, C. D. (1973). An atlas of primate gross anatomy: baboon, chimpanzee, and man. Seattle, WA: Seattle, University of Washington Press.

TOMINAGA, T., DICKMAN, C. A., SONNTAG, V. K., and COONS, S. (1995). Comparative anatomy of the baboon and the human cervical spine. Spine, 20(2): 131-7.

YINGLING, V. R., CALLAGHAN, J. P., and MCGILL, S. M. (1997). Dynamic loading affects the mechanical properties and failure site of porcine spine. Clin Biomech, 12(15): 301-305.

ZHU, Q., OUYANG, J., LU, W., LU, H., LI, Z., GUO, X., and ZHONG, S. (1999). Traumatic instabilities of the cervical spine caused by high-speed axial compression in a human model. An in vitro biomechanical study. Spine, 24(5): 440-444.

DISCUSSION

PAPER: **Effect of Loading Rate on Cervical Spine Compressive Failure Mechanics**

PRESENTER: ***Paul Elias, Applied Biomechanics Lab [University of Washington]***

QUESTION: *Guy Nusholtz, Daimler/Chrysler*
Your rates going from about 5 mm a second to about 5,000. You saw an increase in the mean value somewhere around 30%.

ANSWER: That's right.

Q: So--and that would be consistent with a lot of materials. You just looked at a material. There's nothing really outside of what we would typically see in a lot materials, so that would basically be consistent. Even though you didn't show statistical significance at 5%, it was so close that you would expect--It would be more reasonable to assume that it's most likely that your failure loads actually did increase as you increase the rates.

A: True. And again, it appears as if we would need about 10 specimens to really show that with statistical significance.

Q: And when you say no relationship between failure and displacement, you're talking about the amount of motion that that head makes, that stays approximately the same at each failure point where it drops off?

A: That's true. Essentially, the displacement of the specimen--how much it's been compressed before we see that it's failed is relatively constant.

Q: So, you're--Yes. Basically, you're saying, as I understand it then: You're strain to failure is approximately the same.

A: True.

Q: And, the thing just gets stiffer. The thing just gets stiffer and that's why you end up where you, where the data...

A: True. Yes.

Q: Okay. Thank you.

Q: *Mike Schlict, Medical College of Wisconsin*
Why a nine year-old?

A: Why a nine year-old? Good question. Well, we did want to test in the pediatric range. It actually just so happened that we had the most of that group.

Q: You think that was the reason behind the burst fracture being the primary mode? The nine year-old? Or, that development of the spine that you were testing?

A: To be entirely honest, I really don't know. [It is unclear whether development played a role due to the fact that only 1 age group was tested in this study. A subsequent study varying age and loading rate is in progress to address this question.]

Q: Thank you.

Q: *Erik Takhounts, National Highway Traffic Safety Administration*
I'm surprised with your precondition protocol. Fifty cycles seems to be excessive for an affect caused by positioning. If after 50 cycles, you still have change in force, there is something else that is going on there.

A: Okay. I think 50 cycles was chosen because at the end, we were actually seeing a consistent load displacement curve.

Q: But if you have actual preconditioning affect, then usually for biological tissue you will see 25, 6, 10 cycles. But, 50 cycles seemed to be excessive. I was wondering if you gave it any thought why this happened.

A: I don't know specifically. I do know that this preconditioning was chosen essentially based on other tests that we ran in other modes: tension, sheer. I don't know specifically where those originated and why 50 was chosen. [To date, we have seen no evidence in the literature to suggest that 50 cycles would be harmful to the specimens.]

Q: What usually fails first in compression?

A: What fails first? We don’t know specifically what failed first, but in post-test radiographs we saw mostly burst fractures.

Q: Did you test only one direction and try to rotate it a little and see--?

A: No, we tested only one.

Q: Okay. Thank you.